Available online at www.sciencedirect.com
SCIENCE DIRECT
Biochemical Pharmacology 67 (2004) 2207–2218
Biochemical Pharmacology
www.elsevier.com/locate/biochempharm

Polyhydroxylated 2-styrylchromones as potent antioxidants

Paulo Filipe[a,b], Artur M.S. Silva[c], Patrice Morlière[b], Cristela M. Brito[c], Larry K. Patterson[d,e], Gordon L. Hug[d], João N. Silva[a,b], José A.S. Cavaleiro[c], Jean-Claude Mazière[e], João P. Freitas[a], René Santus[b,*]

[a]*Centro de Metabolismo e Endocrinologia da Faculdade de Medicina de Lisboa, Hospital de Santa Maria, 1699 Lisbon, Portugal*
[b]*INSERM U 532, Institut de Recherche sur la Peau, 1 Avenue Claude Vellefaux, 75475 Paris, Cedex 10, France*
[c]*Department of Chemistry, University of Aveiro, Campus Universitário de Santiago, 3810-193 Aveiro, Portugal*
[d]*Radiation Laboratory, University of Notre Dame, Notre Dame, IN 46556, USA*
[e]*Service de Biochimie, Hôpital Nord d'Amiens, 80054 Amiens, Cedex 01, France*

Received 2 December 2003; accepted 12 February 2004

Abstract

Four polyhydroxylated 2-styrylchromones, structurally related to flavones and cinnamic acid, have been studied. An SC derivative with OH groups only at positions 3′ and 4′ on the styryl moiety and another SC bearing an additional OH group at position 5 on the benzopyrone ring were more potent inhibitors of the Cu^{2+}-induced peroxidation of LDL than the flavonoid quercetin. Fluorescence and absorption spectroscopies suggested that one LDL particle may bind 40 SC molecules. A pulse radiolysis study in pH 7 buffered micellar solutions of neutral TX100 and positively charged CTAB demonstrated that one-electron oxidation by $^{\bullet}Br_2^-$, $^{\bullet}O_2^-$ and tryptophan radicals ($^{\bullet}$Trp) depends strongly on the micellar microenvironment. All SCs were readily oxidized by $^{\bullet}O_2^-$ in CTAB micelles (rate constants: $6–18 \times 10^6$ M^{-1} s^{-1}). In TX100 micelles only the SC derivative with OH groups in position 3′ and 4′ reacted with $^{\bullet}O_2^-$ (rate constant: 1.1×10^6 M^{-1} s^{-1}). In CTAB, electron transfer to $^{\bullet}$Trp radicals was observed for all SCs with rate constants $\geq 3.2 \times 10^7$ M^{-1} s^{-1}. In TX100 micelles, this reaction occurred solely with the derivative bearing OH groups only at positions 3′ and 4′.

Keywords: LDL oxidation; Fast kinetics; Micelles; Pulse radiolysis; Superoxide radical; Tryptophan; Redox reactions

1. Introduction

Reactive oxygen species (ROS) such as $^{\bullet}O_2^-$, $^{\bullet}$OH, and H_2O_2 generated by cellular metabolism or arising from environmental sources (chemicals, UV light) are recognized as factors contributing to major diseases such as atherosclerosis [1], cancer [2], and central nervous system degeneration [3] and are implicated in the general aging process [4]. In addition to the constitutive cell antioxidant defense system, there exist various small molecules, vitamins (ascorbic acid and α-tocopherol), carotenoids, flavonoids and simpler phenolic coumponds, which exhibit potent antioxidant properties and which are excellent reactive oxygen species scavengers. These are essential to good health and are found in large quantities in fruits and vegetables [5,6]. Literature data suggest that antioxidants often work by the combination of several mechanisms such as scavenging of lipid alkoxyl and peroxyl radicals through hydrogen donation, regeneration of α-tocopherol by α-tocopheroxyl radical reduction and chelation of transition metal ions [7]. More recently, the repair of oxidative damage to proteins or lipoproteins has been shown to also contribute to the flavonoid antioxidant activity [8,9].

In practice, the protection afforded by antioxidants against oxidative stress and its consequences to human health are limited. Thus, antioxidants may exhibit pro-oxidant properties under appropriate conditions. Another important factor that limits the efficacy of antioxidants is their bioavailability [10,11]. Consequently, it is of interest to search out new molecules with improved antioxidant properties to help circumvent some limitations of presently available antioxidants.

Abbreviations: CTAB, cetyltrimethylammonium bromide; LDL, low-density lipoprotein; ROS, reactive oxygen species; Q, quercetin; SC, 2-styrylchromone; TX100, Triton X100

* Corresponding author. Tel.: +33-1-40793726; fax: +33-1-40793716.
E-mail address: santus@mnhn.fr (R. Santus).

0006-2952/$ – see front matter © 2004 Elsevier Inc. All rights reserved.
doi:10.1016/j.bcp.2004.02.030

The present study concerns polyhydroxylated SCs. These compounds are structurally related to cinnamic acids and flavones, i.e. two families of molecules which exhibit potent antioxidant properties. To date, only two natural SCs are known [12,13]. However, synthetic molecules of this class of compounds exhibit antiallergic, antitumor, and anticancer properties [12–15]. More specifically, some polyhydroxylated SCs are potent inhibitors of xanthine oxidase [16] and potent hepatoprotectors against *tert*-butylhydroperoxide [17]. Little is known about the biochemical mechanisms responsible for their biological effects.

This study, is therefore, intended to explore possible antioxidant properties of four synthetic SCs substituted with an increasing number of hydroxyl groups on both the chromone and styryl moieties. To this end, we have studied their inhibitory effect on Cu^{2+}-induced oxidation of isolated human serum low-density lipoproteins (LDLs), a well-established in vitro model of lipid peroxidation via radical chain reaction [18]. The formation of conjugated dienes and the consumption of carotenoids were chosen as markers of LDL lipid peroxidation [19]. Their inhibition by polyhydroxylated SCs was compared to that observed in the presence of the flavone quercetin since the latter is known to be an effective inhibitor of the LDL lipid peroxidation [10].

This result prompted us to undertake a more detailed mechanistic study of their antioxidant and redox properties by means of fast kinetics spectroscopy. This subsequent investigation was carried out in neutral Triton X100 (TX100) and cationic cetyltrimethylammonium bromide (CTAB) pH 7 buffered micellar solutions. These two kinds of micelles are related to two important microenvironments found in the LDLs. These are the hydrophobic apolar neutral lipid core and the heavily positively charged apolipoprotein B containing 353 Lys and 152 Arg residues which play a key role in the recognition of the so-called Apo-B/E cell receptor [20]. The apolipoprotein B interacts with the outer layer of phospholipids and cholesterol in contact with the aqueous phase and with the lipidic core of the LDLs. In the TX100 and CTAB micelles, the phenoxyl radicals resulting from the one-electron oxidation of the SCs, by the mildly oxidizing $^{\bullet}Br_2^-$ radical anions, were characterized spectroscopically by pulse radiolysis. Using the spectral data obtained, we demonstrated that polyhydroxylated SCs also react very effectively with the $^{\bullet}O_2^-$ radical anion in these aqueous micellar systems.

Amino acid residues of proteins are also important biological targets of oxidative damage by ROS [21]. The neutral indolyl radical ($^{\bullet}$Trp) is the primary transient species produced by oxidation of the aromatic amino acid Trp, which is among the residues most energetically vulnerable to radical attack. $^{\bullet}$Trp can be produced by strongly oxidizing $^{\bullet}$OH radicals or, more selectively, by milder oxidants such as $^{\bullet}Br_2^-$, $^{\bullet}(SCN)_2^-$, or $^{\bullet}N_3$. Since $^{\bullet}$Trp absorbs in the UV–Vis, its kinetic behavior can be readily monitored [22]. Since oxidized Trp residues in proteins can be repaired by antioxidants such as ascorbate [23] and flavonoids [8,9], repair of $^{\bullet}$Trp was also chosen as a probe of the antioxidant capacity of the SCs studied.

2. Materials and methods

2.1. Chemicals and routine equipment

All routine chemicals were of analytical grade and were used as received from the suppliers. Quercetin, D,L-tryptophan, CTAB, and TX100 were purchased from Sigma. Dimethyl sulfoxide, absolute ethanol, and methanol were supplied by Merck and were of spectroscopic grade. The phosphate buffer (pH 7) was prepared in pure water obtained with a reverse osmosis system from Ser-A-Pure Co. This water exhibits a resistivity of >18 MΩ cm^{-1} and a total organic content of <10 ppb. Solutions were saturated with pure N_2O or O_2. Absorption spectrophotometry was carried out with an Uvikon 943 spectrophotometer whereas fluorescence spectra were recorded with a Shimadzu RF5000 spectrofluorometer.

The polyhydroxylated 2-styrylchromones SC2–SC4 (Scheme 1) were synthesized as described in [24]. 3′,4′-Dihydroxy-2-styrylchromone SC1 was prepared as detailed below and as summarized in Scheme 2.

2.2. Synthesis of 3′,4′-dihydroxy-2-styrylchromone (SC1)

2.2.1. 2′-(3,4-Dibenzyloxycinnamoyloxy)acetophenone (*1*)

3,4-Dibenzyloxycinnamic acid (6.8 g, 18.9 mmol) and phosphorus oxychloride (8.0 ml, 86 mmol) were added to a solution of the 2′-hydroxyacetophenone (2.0 ml, 16.6 mmol) in dry pyridine (300 ml). The solution was stirred at 60 °C for 4 h. Subsequently, the solution was poured into ice and water (200 ml), and the pH adjusted to 4 with hydrochloric acid. The mixture was then extracted with chloroform (2 × 100 ml) and the organic layer washed with water. The solvent was evaporated and the residue was purified by silica gel column chromatography using a (3:7)

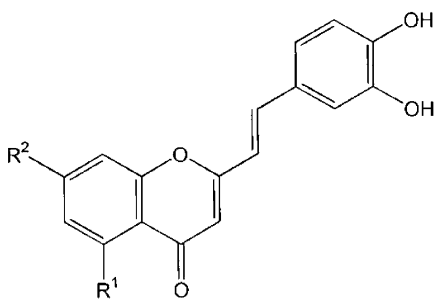

SC1: $R^1 = R^2 = H$ SC2: $R^1 = OH$, $R^2 = H$
SC3: $R^1 = H$, $R^2 = OH$ SC4: $R^1 = R^2 = OH$

Scheme 1.

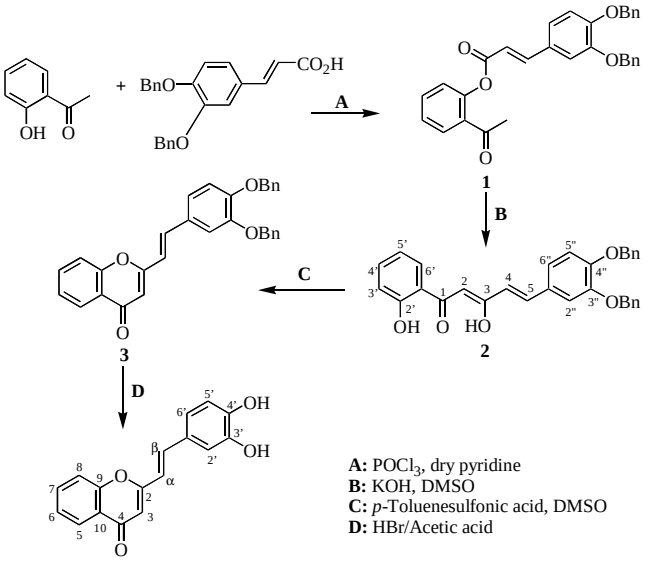

Scheme 2.

mixture of light petroleum:dichloromethane as eluent. This solvent was then evaporated to dryness and the residue was crystallized from ethanol to give 2′-(3,4-dibenzyloxycinnamoyloxy)acetophenone (**1**) (4.6 g, yield: 58%). m.p. 108–109 °C (recrystallized from ethanol). ^{1}H NMR: $\delta = 2.56$ (s, 3H, 2-C*H*$_3$), 5.21 (s, 2H, 3″-OC*H*$_2$C$_6$H$_5$), 5.23 (s, 2H, 4″-OC*H*$_2$C$_6$H$_5$), 6.46 (d, *J* 15.8 Hz, 1H, H-α), 6.94 (d, *J* 8.4 Hz, 1H, H-5″), 7.14 (dd, *J* 8.4 and 2.0 Hz, 1H, H-6″), 7.18 (dd, *J* 7.4 and 1.5 Hz, 1H, H-3′), 7.19 (d, *J* 2.0 Hz, 1H, H-2″), 7.26–7.49 (m, 11H, H-5′ and H-2,3,4,5,6 of 3″,4″-OCH$_2$C$_6$*H*$_5$), 7.56 (dt, *J* 7.4 and 1.6 Hz, 1H, H-4′), 7.78 (d, *J* 15.8 Hz, 1H, H-β), 7.83 (dd, *J* 7.7 and 1.6 Hz, 1H, H-6′). ^{13}C NMR: $\delta = 29.9$ (C-2), 70.9 (4″-O*C*H$_2$C$_6$H$_5$), 71.3 (3″-O*C*H$_2$C$_6$H$_5$), 113.8 (C-2″), 114.1 (C-5″), 114.5 (C-α), 123.5 (C-6″), 123.8 (C-3′), 126.0 (C-5′), 127.1, 127.3, 127.4, and 128.0 (C-2,3,4,5,6 of 3″,4″-OCH$_2$*C*$_6$H$_5$), 130.1 (C-6′), 131.4 (C-1′), 133.3 (C-4′), 136.6 and 136.8 (C-1″ and C-1 of 3″,4″-OCH$_2$*C*$_6$H$_5$), 147.2 (C-β), 148.9 (C-2′), 149.2 (C-3″), 151.5 (C-4″), 165.4 (C=O), 197.9 (C-1). EI-MS: *m*/*z* (%) = 478(7) (M$^{\bullet+}$), 344(9), 343(34), 253(5), 251(3), 181(8), 163(2), 136(3), 121(6), 105(2), 92(11), 91(100), 77(4), 65(9), 63(3), 51(3). C$_{31}$H$_{26}$O$_5$ (478.5): Calc. C, 77.81; H, 5.48. Found C, 77.81; H, 5.40.

2.2.2. 1-(2-Hydroxyphenyl)-5-(3,4-dibenzyloxyphenyl)-3-hydroxy-2,4-pentadiene-1-one (2)

Potassium hydroxide (powder, 1.0 g, 25 mmol) was added to a solution of 2′-(3,4-dibenzyloxycinnamoyloxyacetophenone (**1**) (2.4 g, 5 mmol) in dimethyl sulfoxide (30 ml). The solution was stirred, under nitrogen, at room temperature for 2 h. Following that period the solution was poured into ice and water (200 ml), and the pH was adjusted to 4 with diluted hydrochloric acid. The solid obtained was removed by filtration, dissolved in dichloromethane (20 ml) and purified by silica gel column chromatography using dichloromethane as eluent. This solvent was evaporated to dryness and the residue was then crystallized from ethanol giving 1-(2-hydroxyphenyl)-5-(3,4-dibenzyloxyphenyl)-3-hydroxy-2,4-pentadiene-1-one (**2**) (2.0 g, yield: 84%). m.p. 133–136 °C (recrystallized from ethanol). ^{1}H NMR: $\delta = 5.21$ (s, 2H, 3″-OC*H*$_2$C$_6$H$_5$), 5.22 (s, 2H, 4″-OC*H*$_2$C$_6$H$_5$), 6.28 (s, 1H, H-2), 6.40 (d, *J* 15.7 Hz, 1H, H-4), 6.90 (ddd, *J* 8.5, 7.6 and 1.0 Hz, 1H, H-5′), 6.94 (d, *J* 8.4 Hz, 1H, H-5″), 6.99 (dd, *J* 8.4 and 1.0 Hz, 1H, H-3′), 7.12 (dd, *J* 8.4 and 1.9 Hz, 1H, H-6″), 7.16 (d, *J* 1.9 Hz, 1H, H-2″), 7.30–7.49 (m, 11H, H-4′ and H-2,3,4,5,6 of 3″,4″-OCH$_2$C$_6$*H*$_5$), 7.55 (d, *J* 15.7 Hz, 1H, H-5), 7.69 (dd, *J* 8.5 and 1.5 Hz, 1H, H-6′), 12.27 (s, 1H, 2′-O*H*), 14.72 (s, 1H, 3-O*H*). ^{13}C NMR: $\delta = 70.9$ (4″-O*C*H$_2$C$_6$H$_5$), 71.4 (3″-O*C*H$_2$C$_6$H$_5$), 96.5 (C-2), 113.7 (C-2″), 114.3 (C-5″), 118.7 (C-3′), 119.0 (C-5′), 119.1 (C-1′), 120.1 (C-4), 122.9 (C-6″), 127.2, 127.3, 127.5, 128.0 and 128.4 (C-2,3,4,5,6 of 3″,4″-OCH$_2$*C*$_6$H$_5$), 128.4 (C-6′), 135.7 (C-4′), 136.7 and 136.9 (C-1″ and C-1 of 3″,4″-OCH$_2$*C*$_6$H$_5$), 139.8 (C-5), 149.0 (C-3″), 151.0 (C-4″), 162,5 (C-2′), 174.9 (C-3), 195.6 (C-1). EI-MS: *m*/*z* (%) = 478 (8) (M$^{\bullet+}$), 387(3), 369(2), 181(4), 163(3), 121(18), 92(11), 91(100), 77(2), 65(10), 63(2), 51(2). C$_{31}$H$_{26}$O$_5$ (478.5): Calc. C, 77.81; H, 5.48. Found C, 77.94; H, 5.52.

2.2.3. 3′,4′-Dibenzyloxy-2-styrylchromone (3)

p-Toluenesulfonic acid monohydrate (0.38 g, 2.0 mmol) was added to a solution of 1-(2-hydroxyphenyl)-5-(3,4-dibenzyloxyphenyl)-3-hydroxy-2,4-pentadiene-1-one (**2**) (1.9 g, 4 mmol) in dimethyl sulfoxide (30 ml). This solution was heated, under nitrogen, at 90 °C, until the complete consumption of the starting material. After that period, the solution was poured into ice and water (100 ml) and the solid obtained was removed by filtration. This solid was dissolved in dichloromethane (50 ml) and the organic layer washed with water (2 × 100 ml). After evaporation of the solvent to dryness, the residue was crystallized from ethanol giving 3′,4′-dibenzyloxy-2-styrylchromone (**3**) (1.6 g, yield: 85%). m.p. 161–163 °C (recrystallized from ethanol). ^{1}H NMR: $\delta = 5.22$ (s, 2H, 4′-OC*H*$_2$C$_6$H$_5$), 5.23 (s, 2H, 3′-OC*H*$_2$C$_6$H$_5$), 6.29 (s, 1H, H-3), 6.58 (d, *J* 16.0 Hz, 1H, H-α), 6.96 (d, *J* 8.4 Hz, 1H, H-5′), 7.14 (dd, *J* 8.4 and 2.0 Hz, 1H, H-6′), 7.19 (d, *J* 2.0 Hz, 1H, H-2′), 7.33–7.43 (m, 10H, H-2,3,4,5,6 of 3′,4′-OCH$_2$C$_6$*H*$_5$), 7.48 (dd, *J* 8.3 and 7.6 Hz, 1H, H-6), 7.51 (d, *J* 16.0 Hz, 1H, H-β), 7.52 (d, *J* 8.2 Hz, 1H, H-8), 7.68 (ddd, *J* 8.2, 7.6 and 1.6 Hz, 1H, H-7), 8.20 (dd, *J* 8.3 and 1.6 Hz, 1H, H-5). ^{13}C NMR: $\delta = 71.0$ (4′-O*C*H$_2$C$_6$H$_5$), 71.4 (3′-O*C*H$_2$C$_6$H$_5$), 110.1 (C-3), 113.4 (C-2′), 114.4 (C-5′), 117.8 (C-8), 118.3 (C-α), 122.4 (C-6′), 124.1 (C-10), 124.9 (C-6), 125.6 (C-5), 127.2, 127.3, 128.0 and 128.5 (C-2,3,4,5,6 of 3′,4′-OCH$_2$*C*$_6$H$_5$), 133.6 (C-7), 136.7 (C-β), 136.9 (C-1′), 136.9 (C-1 of 3′,4′-OCH$_2$*C*$_6$H$_5$), 149.1 (C-3′), 150.7 (C-4′), 156.0 (C-9), 162.0 (C-2), 178.4 (C-4). EI-MS: *m*/*z* (%) = 460 (22) (M$^{\bullet+}$), 370(11), 369(23), 352(4),

221(2), 181(3), 121(2), 92(14), 91(100), 65(11), 63(3), 51(2). $C_{31}H_{24}O_4$ (460.5): Calc. C, 80.85; H, 5.25. Found C, 80.84; H, 5.26.

2.2.4. 3′,4′-Dihydroxy-2-styrylchromone (SC1)

3′,4′-Dibenzyloxy-2-styrylchromone (**3**) (1.2 g, 2.55 mmol) was added to a solution of hydrogen bromide in acetic acid (33%, 50 ml). The mixture was refluxed for 2 h. The solution was then carefully poured into ice and water and the solid obtained was removed by filtration. The solid was dissolved in ethyl acetate (20 ml) and washed with water several times. After evaporation of the solvent, this residue was purified by silica gel column chromatography using a (8:2) mixture of chloroform:acetone as eluent. The solvent was evaporated to dryness, and the residue was precipitated from ethanol with water giving 3′,4′-dihydroxy-2-styrylchromone (SC1) (286 mg, yield: 40%). m.p. 176–177 °C. ^{1}H NMR (DMSO-d_6): $\delta = 6.42$ (s, 1H, H-3), 6.79 (d, J 8.2 Hz, 1H, H-5′), 6.88 (d, J 16.0 Hz, 1H, H-α), 7.03 (dd, J 8.2 and 2.0 Hz, 1H, H-6′), 7.11 (d, J 2.0 Hz, 1H, H-2′), 7.46 (ddd, J 7.7, 7.3 and 0.8 Hz, 1H, H-6), 7.55 (d, J 16.0 Hz, 1H, H-β), 7.71 (d, J 8.2 Hz, 1H, H-8), 7.80 (ddd, J 8.2, 7.3 and 1.6 Hz, 1H, H-7), 8.00 (dd, J 7.7 and 1.6 Hz, 1H, H-5) ^{13}C NMR (DMSO-d_6): $\delta = 109.0$ (C-3), 114.3 (C-2′), 115.9 (C-5′), 116.7 (C-α), 118.2 (C-8), 120.9 (C-6′), 123.5 (C-10), 124.8 (C-5), 125.1 (C-6), 126.6 (C-1′), 134.1 (C-7), 137.2 (C-β), 145.7 (C-3′), 148.0 (C-4′), 155.5 (C-9), 162.4 (C-2), 176.9 (C-4). EI-MS: m/z (%) = 280 (100) ($M^{\bullet+}$), 263(29), 251(5), 234(10), 233(11), 223(8), 205(9), 187(13), 160(29), 131(7), 121(47), 114(16), 103(9), 92(13), 84(17), 77(9), 76(9), 66(20), 63(12), 51(7). $C_{17}H_{12}O_4$ (280.3): Calc. C; 72.85; H, 4.32. Found C, 72.82; H 4.33.

2.3. Preparation and treatment of LDL

Serum samples were obtained from healthy volunteers. The LDLs ($d = 1.024-1.050$ g ml^{-1}) were prepared by sequential ultracentrifugation according to Havel et al. [25]. Protein content was determined by the technique of Peterson [26]. The LDL samples were used within 2–3 weeks. Just before experimentation, the LDLs were dialyzed twice for 8 and 16 h against 1 l of 10 mM phosphate buffer (pH 7.4) to remove EDTA. Then, the LDLs were diluted to a final concentration of 0.15 mg ml^{-1} (300 nM). To obtain the desired concentration, the appropriate volume of 0.5 mM 2-styrylchromone (SC) or quercetin (Q) stock solutions in ethanol as well as 150 μl of buffer were added 800 μl of the diluted LDLs. Blank LDL solutions without SC or Q were also prepared. The LDL solutions loaded with SC or Q and the blank LDL solutions were then incubated at 37 °C for 15 min. Lipid peroxidation was triggered by adding 50 μl of $CuCl_2$ to achieve a Cu^{2+} concentration of 5 μM. After Cu^{2+} addition, conjugated diene formation was measured periodically during continuous incubation at 37 °C.

2.4. Conjugated diene determination

Conjugated diene formation was monitored by second derivative absorption spectroscopy (220–300 nm) based on an earlier methodology described in the literature [27]. With protein solutions, second derivative absorption spectroscopy is generally preferred to direct absorption spectroscopy because it is much less sensitive to scattered light. Before recording spectra, 80 μl of the sample were diluted 10-fold with 10 mM phosphate buffer (pH 7.4). The second derivative spectrum was subtracted from the second derivative spectrum of the matching control sample without Cu^{2+}. The increase in conjugated dienes expressed in relative units was obtained from the amplitude of the 254 nm peak.

2.5. Consumption of carotenoids

The basal carotenoid content of LDL preparations was spectrophotometrically determined [28]. The concentration of total carotenoids can be determined using an average extinction coefficient of 140,000 M^{-1} cm^{-1} at 448 nm. This value is based on a calculation of contributions from the four main carotenes in human plasma, β-carotene, β-carotene, β-cryptoxanthin, and lycopene [29]. Changes in carotenoid concentration during LDL oxidation were monitored by second derivative absorption spectroscopy (400–550 nm) through measurement of the second derivative spectrum amplitude between 489 and 516 nm.

2.6. Pulse radiolysis

Pulse radiolysis measurements were carried out with the Notre Dame Radiation Laboratory 8-MeV linear accelerator, which provides 5 ns pulses of up to 30 Gy. In general, the doses used in this work were approximately 2–20 Gy. The principles of the detection system have been previously described [30,31]. A Corning O-51 optical filter, which removes all wavelengths shorter than 350 nm, was placed in the analyzing light beam preceding the sample cell.

Radical concentrations calculated from transient absorption data are referenced to $^{\bullet}(SCN)_2^-$ dosimetry. The extinction coefficient for $^{\bullet}(SCN)_2^-$ is taken to be 7580 ± 60 M^{-1} cm^{-1} at 472 nm, and the G value for $^{\bullet}$OH in N_2O-saturated solution has been measured as 6.13 ± 0.09 [32]. The G value or radiolytic yield is the number of radicals generated per 100 eV of absorbed energy. Such numbers may be recast as radical concentrations per unit radiation (e.g. a G value of 6.1 corresponds to a concentration of ~0.63 μM Gy^{-1}).

Solutions for pulse radiolysis were prepared in 10 mM phosphate buffer solutions (pH 7) of CTAB and TX100. The concentrations used were 10 and 3 mM, respectively, well above the critical micellar concentration for each

surfactant involved. This allows one to assume that most detergent is in micellar form. All solutions also contained 0.1 M Br^- unless otherwise stated. Triton X100 could be used in this work since it was previously shown by one of us that it does not react with $^{\bullet}Br_2^-$ radical anions [33]. To minimize the volumes of SC solutions required, a microcell (optical path: 1 cm, volume: 120 μl and 2 mm i.d. Teflon® tubing) was used for transient recording. Where necessary, differences in radical *G* value, arising from the dependence of spur scavenging on Br^- concentration, are taken into account [34]. Additionally, production of superoxide radical by oxygen scavenging of $H^{\bullet}$ is included in calculating the *G* value for $^{\bullet}O_2^-$. Numerical integrations, applied to the analysis of rate data, were carried out using the Scientist software from Micromath Scientific Software.

3. Results and discussion

3.1. Inhibition of conjugated diene formation by SCs during Cu^{2+}-induced LDL lipid peroxidation

It is common knowledge that LDLs are natural carriers of important antioxidants such as Vitamin E and carotenoids. Because antioxidants compete with LDL lipids for the propagation of the radical chain reactions, a lag time, due to the antioxidant consumption, is observed between the start of the oxidation by Cu^{2+} ions and the appearance of lipid peroxidation products. The duration of this induction period depends on the constitutive antioxidant content of the LDLs which may vary among blood donors [35]. Fig. 1A shows the time course of the conjugated diene formation after addition of Cu^{2+} ions to native LDL and after loading the LDL with 3 μM SC or Q. It may be seen that under these concentration conditions, SC1, SC2, and Q totally inhibit the formation of conjugated dienes for a period of at least 3 h of incubation at 37 °C. On the other hand, SC4 only partially retards the propagation phase, and inclusion of SC3 exhibits only a minimal effect on the kinetics. Thus, as reflected in Cu^{2+}-induced LDL oxidation, only SC1 and SC2 can be considered as antioxidants competitive with Q, one of the most potent antioxidant polyphenols [7,10,36].

To further assess the antioxidant potential of SC1 and SC2 in comparison to that of Q, the concentration threshold was determined at which SC1, SC2, and Q can totally inhibit conjugated diene formation or carotenoid consumption over a standard 3 h period. Fig. 1B demonstrates that SC1 at a concentration of 0.75 μM is the most powerful antioxidant in this model system, whereas SC2 by itself is more potent than Q. A similar order of effectiveness was observed for the inhibition of the carotenoid consumption by the SC derivatives (Fig. 1C).

It should be noted that the present experimental system defines an overall apparent antioxidant capacity. However, these data suggest several structure–activity relationships

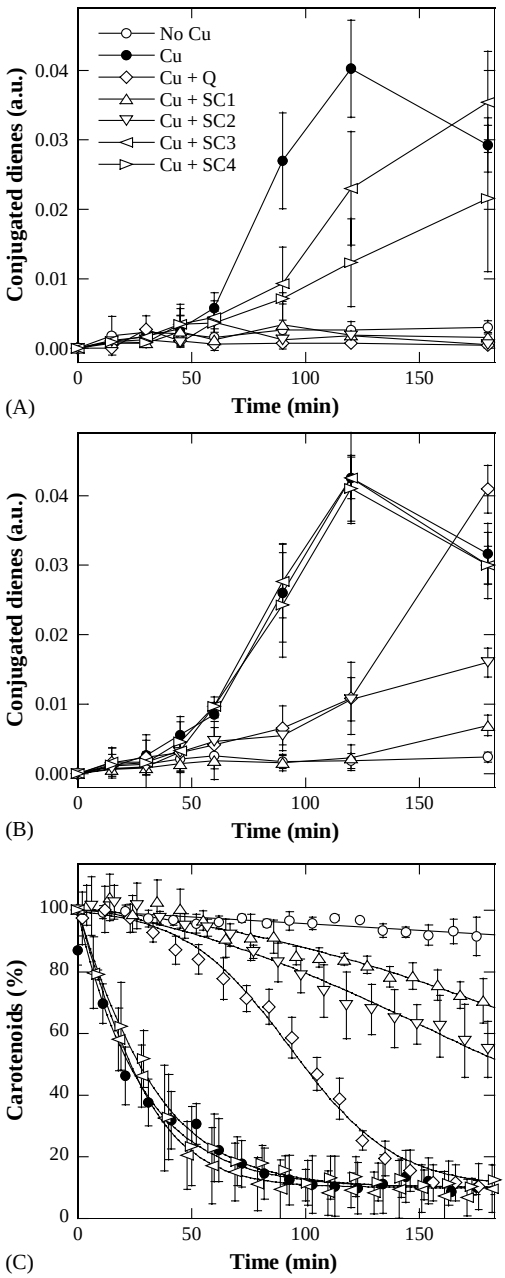

Fig. 1. (A) Kinetics of conjugated diene formation during LDL oxidation induced by 5 μM Cu^{2+}. LDL solutions at 0.12 mg ml^{-1} (240 nM) in 10 mM phosphate buffer (pH 7) were incubated for 15 min at 37 °C with 3 μM SC or Q before Cu^{2+} addition. Note that time zero denotes measurements made at about 1 min after Cu^{2+} addition. Data are the mean ± S.D. of three independent experiments. (B) Same as (A) but the concentrations of SC and Q were 0.75 μM. (C) Kinetics of carotenoid consumption during LDL oxidation induced by 5 μM Cu^{2+}. LDL solutions at 0.12 mg ml^{-1} (240 nM) in 10 mM phosphate buffer (pH 7) were incubated for 15 min at 37 °C with 1.5 μM SC or Q before Cu^{2+} addition. Data are the mean ± S.D. of three independent experiments.

regarding the antioxidant capacity of the SCs investigated. The SC1 derivative with only two OH groups on the styryl moiety is the most effective antioxidant in Cu^{2+}-induced LDL oxidation. Addition of another hydroxyl at position 5 on the benzopyrone ring (SC2 derivative; Scheme 1) leads to less efficient antioxidant behavior. Alternatively, when

there is a single OH group on the benzopyrone ring at position 7, there is a marked decrease in the antioxidant capacity (SC3 derivative). Finally, the behavior of SC4, with two OH substitutions on the benzopyrone ring at positions 5 and 7, is comparable to that of SC3 in antioxidant capacity. Thus, in these systems, increasing the number of hydroxyl groups seems to decrease the antioxidant potential of the SC derivatives. Interestingly, SC4, a rather inactive molecule in this system, has been found to be the most effective xanthine oxidase inhibitor with a 50% inhibition concentration as low as 0.5 μM [16].

This large variation observed in antioxidant effectiveness may be due to different partitioning of the hydrophobic SCs into LDL as a function of the number of their hydroxyl groups present. The interaction of the SCs with the LDL, was therefore, investigated by absorption and fluorescence spectroscopies. Absorption spectroscopy suggests that, like Q [9], the hydrophobic SCs do bind to LDL. Fig. 2A shows that in LDL solutions with the same [LDL]/[SC] ratio as in Fig. 1A, the maximum for SC1 absorbance is shifted to 379 nm—a value approaching those measured in ethanol (380 nm) and methanol (377 nm) (Fig. 2C)—as compared to the value of 373 nm in buffer. Similar data were obtained with the other SCs (data not shown).

Fluorescence studies demonstrate that SC1 is the only fluorescent SC in this study. Fig. 2B displays the fluorescence spectra of 2.5 μM SC1 in ethanol (fluorescence maximum: 520 nm), in pH 7.4, 10 mM phosphate buffer (fluorescence maximum at 527 nm) and in the presence of 100 nM LDL in buffer. Thus, in changing solvent from ethanol to buffer, the SC1 fluorescence is strongly quenched and the maximum is shifted to the red by 7 nm. Addition of 100 nM LDL to the buffer partially restores the SC1 fluorescence and causes significant changes to the spectral shape. The fluorescence maximum is shifted to 475 nm, and a less intense band is observed at about 520 nm, close to the fluorescence maximum found in ethanol. These fluorescence data, along with the absorption spectra, suggest that SC1 does interact with the LDL particle possibly at two different sites.

While the above data point to a possible role for specific LDL-interaction(s) in the antioxidant effectiveness of the SCs, it does not mean that the intrinsic antioxidant potential of these molecules are different. A study of the molecular redox mechanisms underlying the antioxidant activity of the SCs may also contribute to an understanding of the above results. This investigation, presented below, was carried out by pulse radiolysis.

3.2. One-electron oxidation of SCs by pulse radiolysis

The very low solubility of the SCs (approximately 50 μM) in pH 7 phosphate buffer requires the use of solubilizing agents for the study of their redox reactions by pulse radiolysis. Because antioxidants encounter multiple microenvironments under in vivo conditions, micelles

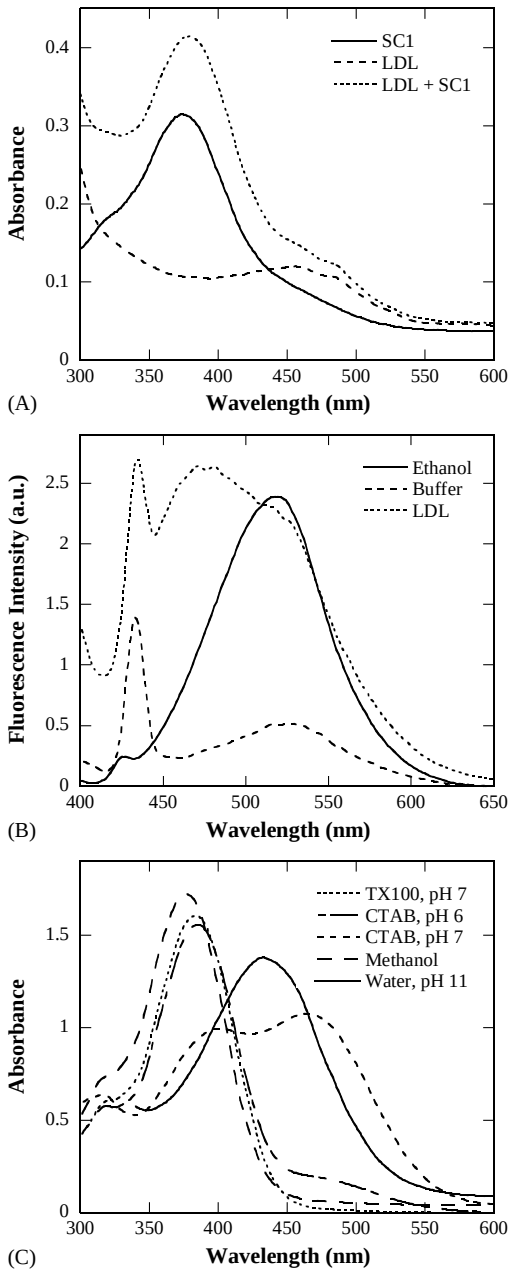

Fig. 2. (A) Absorbance spectra of solutions containing 10 μM SC1 (SC1), 800 nM LDL (LDL), or 800 nM LDL + 10 μM SC1 (LDL + SC1) in 10 mM phosphate buffer (pH 7). Spectra were recorded at 20 °C in 1 cm light-path quartz cells. (B) Fluorescence spectra of solutions of 2.5 μM SC1 in ethanol (ethanol), in 10 mM phosphate buffer, pH 7.4 (buffer) or in the presence of 100 nM LDL in buffer (LDL). Spectra were recorded at 20 °C in 1 cm light-path quartz cells. The excitation wavelength was 375 nm in all cases. Sensitivity has been multiplied by 10 for spectra recorded in buffer and LDL. (C) Absorbance spectra of solutions containing 50 μM SC1 in buffered 1% TX100 containing 10 mM phosphate buffer (TX100, pH 7), in aqueous 10 mM CTAB (CTAB, pH 6), in buffered 10 mM CTAB containing 10 mM phosphate buffer (CTAB, pH 7), in 1 mM aqueous NaOH (water, pH 11) or in methanol (methanol). All spectra were recorded at 25 °C in 1 cm light-path quartz cells.

of differing charge provide good primary model systems for determining environmental effects on radical reactions. Hence, redox reactions of SCs were investigated in solutions containing positively charged CTAB and neutral

TX100 micelles. Furthermore, as indicated in the introduction, they mimic two important microenvironments related to the biological properties of LDLs. For interpretation of radical behavior discussed below, it is first necessary to establish the levels of micellar interaction with SCs.

3.2.1. Influence of bulk pH and of micelle solubilization on spectra of SCs

As suggested by the absorbance measurements carried out in LDL solutions, see above, the optical spectra of all these compounds are sensitive to solvent and microenvironmental factors. Furthermore, the presence of hydroxyl groups leads to pH-dependent absorbance changes. Thus, Fig. 2C reports the absorbance spectra of 50 μM SC1, the simplest polyhydroxylated SC under investigation (see Scheme 1), in methanol, 1% TX100 (pH 7), 10 mM CTAB in water (pH 6), 10 mM CTAB in pH 7 buffer, and 1 mM aqueous NaOH. In these solvents, SC1 as well as SC2, SC3, and SC4 (data not shown) exhibit rather high molar absorbances (approximately about 20,000 $M^{-1}\,cm^{-1}$). In TX100 solution, the SC1 absorbance is similar to that found in methanol which is consistent with the incorporation of SC1 into the polar but uncharged interfacial micellar region. The 59 nm red-shift in the absorbance maximum of SC1 in going from pH 7 (Fig. 2A) to pH 11 (Fig. 2C) reflects the ionization of the hydroxyl groups at the higher pH. As a result, the pH-dependence of the complicated transient spectrum of SC1 in CTAB is consistent with the incorporation of SC1 into the interfacial micellar region where, due to surface electrostatic charges, the pH is raised by about three pH units as compared to the pH of the bulk solution [37]. Fig. 2C shows that the proportion of ionized SC1 molecules increases 5.8 times when the pH of the bulk is raised by one unit. It can be estimated that one of the two OH groups of SC1 has a pK_a of about 9.5. However, the comparison of the spectrum obtained in CTAB with those obtained in methanol and in alkaline aqueous solution demonstrates that other factors specific to the microenvironment such as the polarizability and/or partial solvation in the micellar interior may contribute to the electronic energy of SC1 in CTAB.

3.2.2. Transient absorbance spectra of semi-oxidized SC in micellar media

Pulse radiolysis of a N_2O-saturated buffered aqueous solution containing 0.1 M Br^-, generates $^{\bullet}Br_2^-$ radical anions by the sequence of reactions

$$H_2O \rightarrow e_{aq}^-,\ H^{\bullet},\ {}^{\bullet}OH,\ H_2O_2,\ H_3O^+ \quad (1)$$

$$e_{aq}^- + N_2O + H_2O \rightarrow {}^{\bullet}OH + N_2 + OH^- \quad (2)$$

$$^{\bullet}OH + 2\,Br^- \rightarrow {}^{\bullet}Br_2^- + OH^- \quad (3)$$

The $^{\bullet}Br_2^-$ radical anion is produced with a radiolytic yield of 6.2 (i.e. 0.64 μM Gy^{-1}). In CTAB micelles, after immediate trapping of $^{\bullet}Br_2^-$ by these positively charged micelles, the SCs are readily oxidized by the $^{\bullet}Br_2^-$ radical anions

$$^{\bullet}Br_2^- + SC \rightarrow {}^{\bullet}SC + 2\,Br^- \quad (4)$$

in competition with

$$^{\bullet}Br_2^- + {}^{\bullet}Br_2^- \rightarrow \text{products} \quad (5)$$

In analogy to other phenolic compounds, the hydroxyl groups are probably the electron donating sites for the one-electron oxidation of the SCs. Fig. 3A–D show transient absorbance spectra in the range from 450 to 700 nm obtained at 2 ms after pulse radiolysis of 100 μM SC in pH 7 buffered CTAB and TX100 micellar solutions. These transients all absorb in the 450–700 nm region and all spectra exhibit well-defined peaks. Their spectral shapes remain constant over the 0–200 ms time range (data not shown). The second-order recombination reactions

$$^{\bullet}SC + {}^{\bullet}SC \rightarrow \text{product(s)} \quad (6)$$

occur with rate constants $2k_6$ in the range $(1.1-3.9) \times 10^7\ M^{-1}\,s^{-1}$ in CTAB.

The neutral and ionized forms of the SCs at equilibrium in the CTAB micelles should react differently with $^{\bullet}Br_2^-$ radical anions since phenolates are generally more oxidizable than neutral phenols [38]. As a result, it may be expected that in CTAB both the neutral and ionized species contribute to the overall transient spectra. The rate constants for the formation of the $^{\bullet}SC$ radicals (k_4) were measured by following the growth kinetics of these radicals at the corresponding absorption maxima. These rate constants are all approximately $(6.5-10.6) \times 10^8\ M^{-1}\,s^{-1}$.

As can be seen in Fig. 3A–D, the transient spectra, recorded in neutral TX100 micelles after the one-electron oxidation of 100 μM SC by $^{\bullet}Br_2^-$, are characterized by much weaker transient absorbances than those of the corresponding spectra in CTAB. Additionally, the values of k_4 are smaller ($k_4 = 1.7 \times 10^7\ M^{-1}\,s^{-1}$ for SC1). As indicated in Fig. 2C, the neutral SC species is the one predominantly found in TX100 micelles. This may be reflected both in lower reactivity toward $^{\bullet}Br_2^-$ and in weaker absorbance. Under these conditions, $^{\bullet}Br_2^-$ mainly disappears via reaction (5).

3.2.3. One-electron oxidation of SCs by the $^{\bullet}O_2^-$ radical anion

In biological systems, the presence of O_2 with the attendant formation of $^{\bullet}O_2^-$, via reactions such as (7) and (8) below, adds complexity to the radical kinetics. Antioxidants such as flavonoids are known to react slowly with $^{\bullet}O_2^-$ in homogeneous aqueous solutions [39]. Given that SC1 and SC2 are more effective than Q in the protection of LDL against Cu^{2+}-induced oxidation and given that $^{\bullet}O_2^-$ might be involved as an intermediate [39,40], the presence of $^{\bullet}O_2^-$ must be taken into account. Here $^{\bullet}O_2^-$ reactivity with the SCs in CTAB and TX100

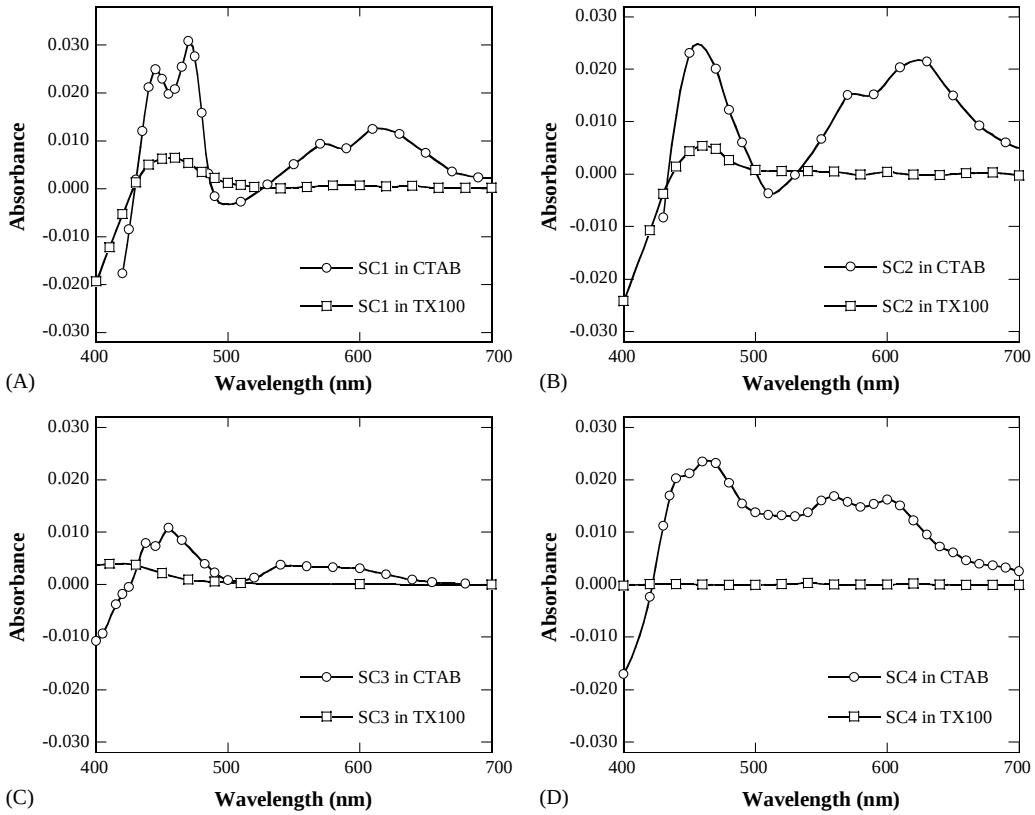

Fig. 3. Transient absorption spectra obtained 2 ms after the radiolytic pulse in N_2O-saturated, 10 mM phosphate buffer (pH 7) containing 0.1 M KBr and either 10 mM CTAB (○) or 3 mM TX100 (□) in the presence of 100 μM SC. (A) SC1, (B) SC2, (C) SC3, and (D) SC4. Note the bleaching below 450 nm due to SC depletion. Dose was 8 Gy.

micelles was measured by pulse radiolysis of O_2-saturated micellar solutions containing 10 mM phosphate buffer (pH 7), 500 μM SC and 0.1 M $HCOO^-$. Under these conditions, all radicals produced by water radiolysis are converted into $^\bullet O_2^-$ radical anions with $G(^\bullet O_2^-) = 6.3$ (0.65 μM Gy^{-1}) by the reactions

$$e_{aq}^- + O_2 \rightarrow {}^\bullet O_2^- \quad (7)$$

$$H^\bullet + O_2 \rightarrow {}^\bullet O_2^- + H^+ \quad (8)$$

$$^\bullet OH + HCOO^- \rightarrow {}^\bullet CO_2^- + H_2O \quad (9)$$

$$^\bullet CO_2^- + O_2 \rightarrow {}^\bullet O_2^- + CO_2 \quad (10)$$

In CTAB micelles all the SCs are readily oxidized by $^\bullet O_2^-$. On the other hand, in the TX100 micelles, only SC1 showed measurable reactivity with $^\bullet O_2^-$. This result was not unexpected in TX100 micelles in view of the found limited reactivity of the SCs with $^\bullet Br_2^-$, a stronger oxidant than $^\bullet O_2^-$. The transient spectra obtained following the oxidation of SC1, SC2, SC3, and SC4 by $^\bullet O_2^-$ in CTAB are shown on Fig. 4A. The spectral shapes and positions of absorbance maxima of these transients are similar to those shown in Fig. 3A–D. However, differences in the ratio of absorbances at wavelengths of maximum absorbance in the blue and red regions are sometimes observed in the spectra taken in CTAB compared to those in TX100. This behavior may reflect differences in the relative reactivity of $^\bullet Br_2^-$ and $^\bullet O_2^-$ with the SC species whose ionic equilibrium is governed by the micellar microenvironment. Assuming full $^\bullet O_2^-$ scavenging by the SCs, an estimate of the molar absorbances of the $^\bullet$SC radicals has been determined (Table 1).

Table 1
Molar absorbance (ε) of $^\bullet$SC radicals obtained by one-electron oxidation of SC by $^\bullet O_2^-$ and reaction rate constants (k_{11}) for the reaction of SC with $^\bullet O_2^-$

Compounds	Conditions	Wavelength (nm)	ε (M^{-1} cm^{-1})	k_{11} ($\times 10^7$ M^{-1} s^{-1})
SC1	CTAB, $^\bullet O_2^-$	600	6100	1.4
SC2	CTAB, $^\bullet O_2^-$	630	7400	1.1
SC3	CTAB, $^\bullet O_2^-$	550	4500	0.6
SC4	CTAB, $^\bullet O_2^-$	560	6400	1.8
SC1	TX100, $^\bullet O_2^-$	460	ND (see text)	0.11

ND: not determined. Temperature was 25 °C. ε and k_{11} values were determined in 10 mM phosphate buffer (pH 7). SC concentration was 250 μM. Dose was about 6 Gy.

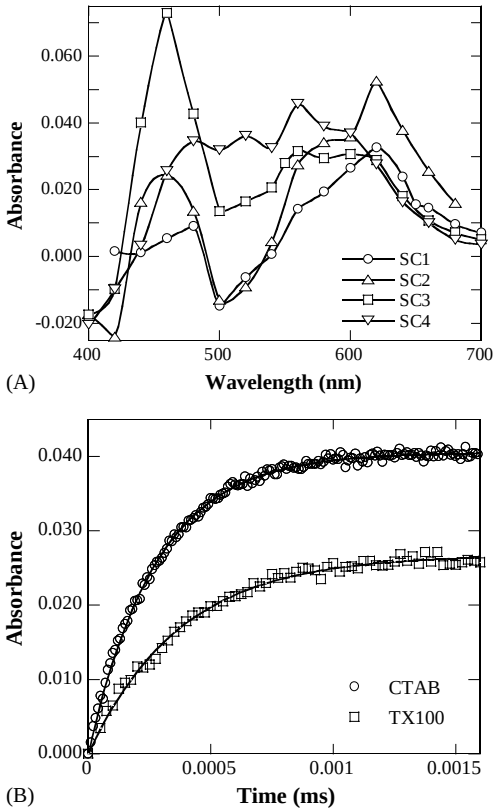

Fig. 4. (A) Transient absorption spectra obtained 2 ms after the radiolytic pulse of O_2-saturated, 10 mM phosphate buffer (pH 7) containing 0.1 M $HCOO^-$ and 10 mM CTAB in the presence of (○) 125 μM SC1, (△) 500 μM SC2, (□) 250 μM SC3, or (▽) 70 μM SC4. Dose was 10 Gy. Note the bleaching of SC below 450 nm. (B) Growth of $^\bullet$SC1 radicals in O_2-saturated 10 mM phosphate buffered micellar solutions (pH 7) containing 0.1 M sodium formate and 250 μM SC1 in the presence of either 10 mM CTAB (○) or 3 mM TX100 (□). Transient growth was recorded at 460 nm. Solid line: fit of the growths assuming pseudo-first-order reaction for SC1 reacting with $^\bullet O_2^-$ (see text). Dose was about 10 Gy. For TX100, absorbances were multiplied by 10 and the time scale by 0.1.

The reaction rate constants, k_{11}, for the oxidation of SC by $^\bullet O_2^-$ depicted by the reaction

$$^\bullet O_2^- + \mathrm{SC} \rightarrow {}^\bullet\mathrm{SC} \quad (11)$$

were calculated from the pseudo-first-order growth kinetics of $^\bullet$SC radicals in CTAB and TX100 micelles (Fig. 4B) and are included in Table 1. The k_{11} values found here in CTAB micelles are comparable to the value measured for $^\bullet$Q formation under similar experimental conditions [8]. The rate constant for the reaction of SC1 and $^\bullet O_2^-$ is 13 times higher in CTAB than in TX100 micelles (Fig. 4B, Table 1). As with other species bearing negative charge such as $^\bullet Br_2^-$, the $^\bullet O_2^-$ radical is most likely localized in the positively charged headgroup region of CTAB, thereby increasing the local concentration of reactants. No effect of this nature is expected or observed with TX100. Furthermore, as discussed above, it is likely that the ionized hydroxyl groups of the SCs in the CTAB micellar solution are much more oxidizable than the un-ionized SCs found in TX100.

3.2.4. Repair of the $^\bullet$Trp radical by SC

Pulse radiolysis of 5 mM Trp in N_2O-saturated micellar solutions of CTAB at pH 7, generates the neutral $^\bullet$Trp radical by the one-electron oxidation reaction

$$^\bullet Br_2^- + \mathrm{Trp} \rightarrow {}^\bullet\mathrm{Trp} + H^+ + 2Br^- \quad (12)$$

In the CTAB micellar solution, the stoichiometric reaction of the $^\bullet Br_2^-$ radical with a large excess of Trp occurs within a few milliseconds with a rate constant $k_{12} = 8.6 \times 10^8\ M^{-1}\ s^{-1}$. This reaction generates the characteristic neutral $^\bullet$Trp radical transient absorption with a maximum at 520 nm ($\varepsilon_{max} = 1750\ M^{-1}\ cm^{-1}$) and negligible absorption beyond 580 nm [22]. The $^\bullet$Trp radical is produced with a G value of 6.2, corresponding to full scavenging of the $^\bullet Br_2^-$ radicals by Trp [8]. As shown in Fig. 5A, the $^\bullet$Trp transient subsequently undergoes bimolecular

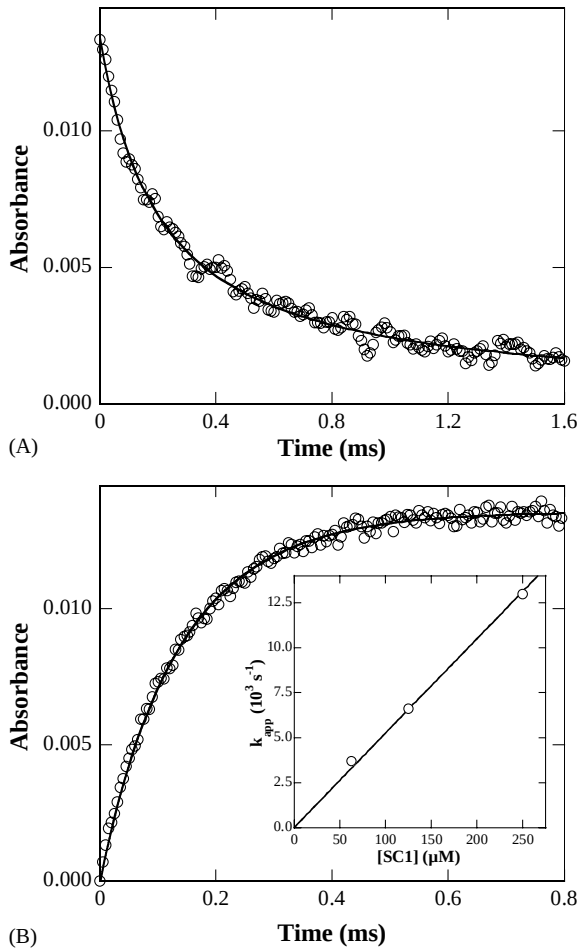

Fig. 5. (A) Decay of the $^\bullet$Trp radical at 520 nm in absence of SC after pulse radiolysis of 5 mM Trp in N_2O-saturated, 10 mM phosphate buffer (pH 7) containing 0.1 M KBr and 10 mM CTAB at 25 °C. Dose was about 12 Gy. Solid line: fit of the $^\bullet$Trp decay to a bimolecular second-order kinetics. (B) Growth of the $^\bullet$SC1 radical at 600 nm with the same constituents as in (A) but in the presence of 125 μM SC1. Solid line: fit of the growth assuming a pseudo-first-order reaction between $^\bullet$Trp and SC1 competing with the $^\bullet$Trp recombination (see text for details). Insert: plot of the pseudo-first-order rate constant (k_{app}) measured from growths recorded at 600 nm as a function of [SC1]. Dose was about 6 Gy.

decay ($2k_{13} = 6.0 \times 10^8\ M^{-1}\ s^{-1}$) [9] according to the reaction

$$2^{\bullet}Trp \rightarrow products \quad (13)$$

Upon addition of 250 μM SC1 to a CTAB micellar solution containing 5 mM Trp, strong transient absorbance changes are observed on a time scale of several hundred microseconds yielding the transient spectrum attributed to the $^{\bullet}$SC1 radical shown in Fig. 3A. Fig. 5B illustrates the slow transient growth at 600 nm, the wavelength maximum of the $^{\bullet}$SC1 radical in the red region. Similar long term radical formation is observed with all SCs (data not shown). The formation of the $^{\bullet}$SC1 radical over such a long time scale cannot be due to the direct reaction of $^{\bullet}Br_2^-$ with SC1 (reaction 4) since all $^{\bullet}Br_2^-$ radical anions react with Trp within a few microseconds. This behavior may, however, be explained by the electron transfer reaction

$$^{\bullet}Trp + SC \rightarrow {}^{\bullet}SC + Trp \quad (14)$$

occurring with the rate constants k_{14} or k_{ET}. The electron transfer yield from SC, measured 500 μs after the pulse, may be seen to approach the G value for the $^{\bullet}$Trp radical production. Tryptophan itself is soluble (~10 mM) in the buffer, and therefore, predominantly in the aqueous phase of micellar solutions. The inset in Fig. 5B, showing the growth rate of the 600 nm transient as a function of the SC1 concentration, demonstrates the pseudo-first-order nature of the $^{\bullet}$SC1 growth which is in agreement with the large excess of SC1 compared to the $^{\bullet}$Trp concentration. The excellent fit of the transient growth at 600 nm (Fig. 5B) has been obtained assuming that the reaction of SC with the $^{\bullet}$Trp radical competes with the bimolecular $^{\bullet}$Trp reaction (reaction 13) illustrated in Fig. 5A. The associated kinetics of $^{\bullet}$Trp and $^{\bullet}$SC can be represented by the equations

$$-\frac{d[^{\bullet}Trp]}{dt} = 2k_{13}[^{\bullet}Trp]^2 + k_{ET}[SC][^{\bullet}Trp]$$

$$\frac{d[^{\bullet}SC]}{dt} = k_{ET}[SC][^{\bullet}Trp]$$

where $2k_{13} = 6.0 \times 10^8\ M^{-1}\ s^{-1}$ and [SC] was varied between 62 and 250 μM.

Table 2
Rate constant (k_{ET}) for the electron transfer from SC to $^{\bullet}$Trp radicals in N_2O-saturated pH 7 buffered micellar solutions

Compounds	Conditions	k_{ET} ($\times 10^7\ M^{-1}\ s^{-1}$)
SC1	CTAB	5.2
SC2	CTAB	4.5
SC3	CTAB	3.2
SC4	CTAB	3.6
SC1	TX100	2.2

Temperature was 25 °C. Pseudo-first-order decays (see text and insert of Fig. 5B) were determined for successive dilutions of a micellar solution containing 250 μM SC and 5 mM Trp with a 5 mM Trp stock micellar solution.

Values of k_{ET} greater than $1 \times 10^7\ M^{-1}\ s^{-1}$ for all the SCs are obtained in a similarly straightforward manner and are compiled in Table 2. It can be seen that these values are rather similar to those previously obtained with Q in CTAB micellar solutions [8]. The repair reaction is also observed with SC1 and $^{\bullet}$Trp in TX100 micelles confirming that the SCs under study are antioxidants at least potentially as good as Q, the reference flavonoid antioxidant.

4. Conclusion

Both the SC1 derivative, with two OH groups on the styryl moiety, and SC2, which has an additional hydroxyl group at position 5 on the benzopyrone ring, compare favorably to quercetin in the protection of LDL lipids from peroxidation in Cu^{2+}-induced oxidation. The study of the electron donating properties of the four SCs by pulse radiolysis in micellar solutions demonstrates that they are equally capable of reacting with $^{\bullet}O_2^-$ and of repairing $^{\bullet}$Trp radicals in CTAB micelles. In such micelles, bearing positively charged head groups, the effectiveness of electron transfer reactions strongly depends on microenvironmental factors such as local pH and electrostatic interactions which modify both the redox parameters and the accessibility (local concentration) of radicals to these hydrophobic SCs. Such factors are also commonly encountered in the control of structure and function in proteins. The superiority of SC1 over the other three SCs is made clear when electron transfer reactions are carried out in neutral TX100 micelles in which SC1 is the sole SC derivative exhibiting measurable reactivity. This observation may be related to the better protection afforded specifically by this antioxidant in the oxidation of LDL by Cu^{2+} ions at pH 7. In this regard, the repair of $^{\bullet}$Trp by SCs suggests that it would be interesting to study the protection brought by SCs against the oxidation of key residues of LDL apolipoprotein B. As a matter of fact, the binding of LDL to their cell receptors requires the integrity of apolipoprotein B. However, other factors must also be taken into account when considering the antioxidant capacity of SCs. Among them, chelation of transition metal ions by SCs should not be ignored since it is believed that the chelating properties of related antioxidants such as flavonoids contribute to their antioxidant activity. Thus, Brown et al. demonstrated that the phenolics that had the greatest propensity for Cu^{2+} ion chelation were the most effective in inhibiting LDL oxidation in the model of copper-mediated LDL oxidation. Their study also showed a significant correlation between partition of phenolics and the inhibition of propagation rate due to redox reactions generated by the hydrophilic Cu^{2+} [41]. Similar factors could play a role in the antioxidant activity of the SCs. Finally, it may also be deduced from this study that the antioxidant potential of the 2-styrylchromones is not necessarily correlated to the number of OH substitutions.

Acknowledgments

This work was supported by an INSERM/GRICES Franco-Portuguese exchange program. J.N.S. thanks the Gulbenkian Foundation for a travel grant and C.M.B. thanks the Organic Chemistry Research Unit and the University of Aveiro for a research grant. We wish to thank Mrs. J. Haigle for her skillful technical assistance. Notre Dame Radiation Laboratory is supported by the Office of Basic Energy Sciences of the US Department of Energy. This is document NDRL-4480 from the Notre Dame Radiation Laboratory.

References

[1] Steinbrecher UP, Zhang H, Lougheed M. Role of oxidatively modified LDL in atherosclerosis. Free Radic Biol Med 1990;9:155–68.
[2] Trush MA, Kensler TW. Role of free radicals in carcinogen activation. In: Sies H, editor. Oxidative stress. Oxidants and antioxidants. San Diego: Academic Press; 1991. p. 277–318.
[3] Mattson MP, Duan W, Pederson WA, Culmsee C. Aging alters the apoptotic response to genotoxic stress. Apoptosis 2001;6:69–81.
[4] Melow S, Ravenscroft J, Malik S, Gill MS, Walker DW, Clayton PE, et al. Extension of life span with superoxide dismutase. Science 2000;289:1567–9.
[5] Halliwell B. Antioxidant defence mechanisms: from the beginning to the end (of the beginning). Free Radic Res 1999;31:261–72.
[6] Hermann K. Occurrence and content of hydroxycinnamic acid and hydroxybenzoic compounds in foods. Crit Rev Food Sci Nutr 1989;28:315–47.
[7] Rice-Evans CA, Miller J, Paganga G. Structure–antioxidant activity relationships of flavonoids and phenolic acids. Free Radic Biol Med 1996;20:933–56.
[8] Filipe P, Morlière P, Patterson LK, Hug GL, Mazière J-C, Mazière C, et al. Mechanisms of flavonoid repair reactions with amino acid radicals in models of biological systems: a pulse radiolysis study in micelles and human serum albumin. Biochim Biophys Acta 2002;1572:150–62.
[9] Filipe P, Morlière P, Patterson LK, Hug GL, Mazière JC, Mazière C, et al. Repair of amino acid radicals of apolipoprotein B100 of low-density lipoproteins by flavonoids. A pulse radiolysis study with quercetin and rutin. Biochemistry 2002;41:11057–64.
[10] Manach C, Morand C, Crespy V, Demigné C, Texier O, Régérat F, et al. Quercetin is recovered in human plasma as conjugated derivatives which retain antioxidant properties. FEBS Lett 1998;426:331–6.
[11] Peng HW, Cheng FC, Huang YT, Chen CF, Tsai TH. Determination of naringenin and its glucuronide conjugate in rat plasma and brain tissue by high-performance liquid chromatography. J Chromatogr B 1998;714:369–74.
[12] Gerkick WH. 6-Desmethoxyhormothamnione, a new cytotoxic styrylchromone from marine cryptophyte *chrysophaeum tailori*. J Nat Prod 1989;22:252–6.
[13] Gerwick WH, Lopez A, Van Duyne V, Clardy J, Ortiz W, Baez A. Hormothamnione, a novel cytotoxic styrylchromone from the marine cyanophyte *Hormothamnion enteromorphoides* Grunow. Tetrahedron Lett 1986;27:1979–87.
[14] Brion JD, Le Baut G, Zammattio F, Pierre A, Atassi G, Belachmi L. Preparation of 2-styryl-4-chromanones as anti-cancer agents. European Patent Applied EP 1991,454,587 [Chem Abstr 1992;116:755 (106092K)].
[15] Doria G, Romeo C, Forgione A, Sberze P, Tibolla N, Cormo ML, et al. Antiallergic agents. III. Substituted *trans*-2-ethenyl-4-oxo-4H-1-benzopyran-6-carboxylic acids. Eur J Med Chem—Chim Ther 1979;27:347–51.
[16] Fernandes E, Carvalho M, Silva AMS, Santos CMM, Pinto DCGA, Cavaleiro JAS, et al. 2-Styrylchromones as novel inhibitors of xanthine oxidase. A structure–activity study. J Enzyme Inhib Med Chem 2002;17:45–8.
[17] Fernandes E, Carvalho M, Carvalho F, Silva AMS, Santos CMM, Pinto DCGA, et al. Hepatoprotective activity of polyhydroxylated 2-styrylchromones against *tert*-butylhydroperoxide induced toxicity in freshly isolated rat hepatocytes. Arch Toxicol 2003;77:500–5.
[18] Rice-Evans CA, Leake D, Bruckdorfer R, Diplock AT. Practical approaches to low-density lipoprotein oxidation: whys, wherefores and pitfalls. Free Radic Res 1996;25:285–311.
[19] Patel RP, Darley-Usmar VM. Molecular mechanisms of the copper dependent oxidation of low-density lipoproteins. Free Radic Res 1999;30:1–9.
[20] Cladaras C, Hadzopoulou-Cladaras M, Nolte RT, Atkinson D, Zannis VI. The complete sequence and structural analysis of human apolipoprotein B-100: relationship between apoB-100 and apoB-48 forms. EMBO J 1986;5:3495–507.
[21] Davies KJA. Protein damage and degradation by oxygen radicals. J Biol Chem 1987;262:9895–901.
[22] Redpath JL, Santus R, Ovadia J, Grossweiner LI. The oxidation of tryptophan by radical anions. Int J Radiat Biol 1975;27:201–4.
[23] Jovanovic SV, Simic MG. Repair of tryptophan radicals by antioxidants. J Free Radic Biol Med 1985;1:125–9.
[24] Santos CMM, Silva AMS, Cavaleiro JAS. Synthesis of new hydroxy-2-styrylchromones. Eur J Org Chem 20034575-4585.
[25] Havel JR, Edre HA, Bragdon J. The distribution and chemical composition of ultracentrifugally-separated lipoproteins in human serum. J Clin Invest 1955;34:1345–53.
[26] Peterson GL. Simplification of the protein assay method of Lowry et al. which is more generally applicable. Anal Biochem 1977;83:346–56.
[27] Corongiu FP, Banni S, Dessi MA. Conjugated dienes detected in tissue lipid extracts by second derivative spectrophotometry. Free Radic Biol Med 1989;7:183–6.
[28] Behrens WA, Thompson JN, Madère R. Distribution of alpha-tocopherol in human plasma lipoproteins. Am J Clin Nutr 1982;35:691–6.
[29] Thurnham DI, Smith E, Flora PS. Concurrent liquid-chromatography assay of retinol, α-tocopherol, β-carotene, α-carotene, lycopene and β-cryptoxanthin in plasma, with tocopherol acetate as internal standard. Clin Chem 1988;34:377–81.
[30] Patterson LK, Lilie JA. Computer-controlled pulse radiolysis system. Int J Radiat Phys Chem 1974;6:129–41.
[31] Hug GL, Wang Y, Schoneich C, Jiang PY, Fessenden RW. Multiple time scale in pulse radiolysis: application to bromide solutions and dipeptides. Radiat Phys Chem 1999;54:559–66.
[32] Schuler RH, Patterson LK, Janata E. Yield for the scavenging of OH radicals in the radiolysis of N_2O-saturated aqueous solutions. J Phys Chem 1980;84:2088–9.
[33] Chauvet JP, Viovy R, Land EJ, Santus R, Truscott TG. One-electron oxidation of carotene and electron transfers involving carotene cations and chlorophyll pigments in micelles. J Phys Chem 1983;87:592–601.
[34] La Verne JA, Pimblott SM. Scavenger and time dependence of radicals and molecular products in the electron radiolysis of water: examination of experiments and models. J Phys Chem 1991;95:3196–206.
[35] Esterbauer H, Striegl G, Puhl H, Rotheneder M. Continuous monitoring of in vivo oxidation of human low density lipoprotein. Free Rad Res Commun 1989;6:67–75.
[36] Bors W, Heller W, Michel C, Saran M. Flavonoids as antioxidants: determination of radical-scavenging efficiencies. Methods Enzymol 1990;186:343–55.
[37] Fernández MS, Fromherz P. Lipoid pH indicators as probes of electrical potential and polarity in micelles. J Phys Chem 1977;81:1755–61.
[38] Jovanovic SV, Steenken S, Simic M, Hara Y. Antioxidant properties of flavonoids: reduction potentials and electron transfer reactions of

flavonoid radicals. In: Rice-Evans CA, Packer L, editors. Flavonoids in health and disease. New York: Marcel Dekker; 1998. p. 137–61.
[39] Perugini C, Seccia M, Bagnati M, Cau C, Albano E, Bellomo G. Different mechanisms are progressively recruited to promote Cu(II) reduction by isolated human low density lipoprotein undergoing oxidation. Free Radic Biol Med 1998;25:519–28.
[40] Pecci L, Montefoschi G, Cavallini D. Some new details on the copper–hydrogen peroxide interaction. Biochem Biophys Res Commun 1997;235:264–7.
[41] Brown JE, Khodr H, Hider RC, Rice-Evans CA. Structural dependence of flavonoid interactions with Cu^{2+} ions: implications for their antioxidant properties. Biochem J 1998;330:1173–8.